

Study of lower emittance dedicated synchrotron radiation mode for the BEPC II *

WANG Dou(王逗) QIN Qing(秦庆) GAO Jie(高杰)

Institute of High Energy Physics, CAS, Beijing 100049, China

Abstract In this paper, a dedicated synchrotron radiation (SR) mode for the BEPC II with an emittance of 85 nm has been designed, including the linear lattice, chromaticity correction and dynamic aperture optimization. The emittance of the new mode is about 60% of the previous mode used for routine operation of the BEPC II. The effect of wigglers on the linear lattice was compensated and the total dynamic aperture including the wigglers' nonlinear effect was estimated. The preliminary commissioning at the end of 2008 and the formal operation with the new mode confirmed its merits.

Key words BEPC II, lower emittance, dedicated SR mode

PACS 29.20.db

1 Introduction

The BEPC II is an upgrade project of the BEPC (Beijing Electron-Positron Collider). This machine is operated not only as an advanced electron-positron collider at the τ -charm energy region but also as a dedicated synchrotron radiation facility at the beam energy of 2.5 GeV. The BEPC II contains a linac, two transport lines and three storage rings. Among three rings, two are for electron and positron beams and two half outer rings are connected as the third ring for the dedicated SR mode through two superconducting dipole coils in the interaction region. There are in total 9 beam lines extracted from 5 wigglers, and 6 from bending magnets, as shown in Fig. 1, where 1W1, 1W2 and so on are the names of the wigglers.

In the BEPC II, high energy physics experiments are prior to SR experiments and the requirement for large emittance and good flexibility made us choose a FODO lattice in the arcs. But for the dedicated SR mode, the emittance should be as small as possible to improve its brightness. Although we have got very good results during the past two years' operation with the previous SR mode, we still need to study the lower emittance mode to improve the performance of the BEPC II as a light source. Since the emittance is determined by the H function when the energy and bending curvature of the machine are

fixed, the only way for us is to reduce the H function in all dipoles. Overall, we can do this by increasing the working points. But it is difficult to do so, due to the limit of the quadrupole strengths of the BEPC II. With effort, we finally reduced the emittance of the dedicated SR mode from the present value of 147 nm to 85 nm.

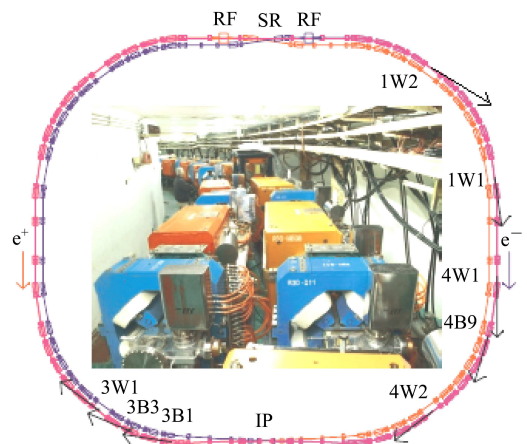


Fig. 1. Layout of the BEPC II storage rings.

2 Linear lattice design

Working point choice always goes first for the lattice design. The working points should be far away

Received 23 October 2009, Revised 8 July 2010

* Supported by National Natural Science Foundation of China (10525525, 10775154)

©2010 Chinese Physical Society and the Institute of High Energy Physics of the Chinese Academy of Sciences and the Institute of Modern Physics of the Chinese Academy of Sciences and IOP Publishing Ltd

from the lowest order resonance lines to avoid potential instabilities. With the consideration of increasing the tunes as many as possible within the limits of quadrupole strengths, we tried $\nu_x/\nu_y=7.28/5.18$, $7.38/5.14$ and $7.72/4.75$, respectively, and finally chose $7.72/4.75$ as the working points with respect to the smallest emittance we could get.

After the working points were fixed, we did some match with the aim of reducing the H function. The expression for the H function is

$$H = \gamma_x D_x^2 + 2\alpha_x D_x D'_x + \beta_x D_x'^2, \quad (1)$$

where α_x , β_x and γ_x are the horizontal twiss parameters, D_x is the horizontal dispersion and D'_x is its deviation.

In the process of matching, several criteria should be considered. First, the horizontal phase advance between the two injection kickers should be π in order to mitigate the disturbance to the circulating beam. Then the horizontal beta functions at the two kickers should be larger than 9 m. For the injection point, the horizontal beta function should be larger than 22 m, the vertical beta function should be larger than 6 m, and the horizontal dispersion is better to be smaller than 0.8 m. Finally, at the positions of the RF cavity, the beta functions should be smaller than 15 m and the horizontal dispersion should be smaller than

0.4 m. In addition, we kept the symmetry of the two kickers in order to control the residual oscillation. The H functions at the center of all the dipoles for both the old and the new modes are shown in Fig. 2.

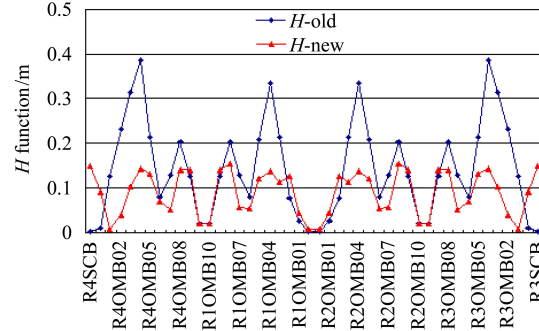


Fig. 2. H functions at the center of all the dipoles for both the old and the new modes.

From Fig. 2, we can see that the average H function in the dipoles for the new mode is apparently smaller than the old one. Fig. 3 shows the twiss parameters for the new mode. Table 1 gives a comparison of the main parameters for these two modes. We can see that the new mode can keep the main original lattice parameters unchanged basically, except for the new working points and the lower emittance.

Table 1. Comparison of the main parameters between the old and the new modes.

	old mode	new mode
working point $\nu_x/\nu_y/\nu_s$	7.28/5.18/0.037	7.72/4.75/0.032
$\varepsilon_{x0}/(\text{nm}\cdot\text{rad})$	146.9	84.5
average H function at the centre of wigglers/m	0.142469	0.089971
momentum compaction factor	0.0186	0.0137
natural energy spread ($\times 10^{-4}$)	6.53	6.56
bunch length/cm	1.24	1.06
natural chromaticity	-9.04/-8.95	-9.81/-8.30
$\beta_{\text{max}}/\text{m}$	22.9/25.0	24.0/24.0
average D_x/m	0.795	0.724
β_x at two kickers/m	10.515	9.00
β at the injection point/m	22.7/14.6	22.8/10.6
D_x at the injection point/m	0.746	0.538
β at RF cavity/m	10.9/16.3	11.3/14.3
D_x at RF cavity/m	0.265	0.400
β at 4W1/m	10.6/24.5	11.0/18.8
β at 4W2/m	5.15/3.35	6.40/ 4.96
β at 1W1/m	7.60/8.61	6.74/ 11.7
β at 1W2/m	4.99/2.17	5.74/ 3.51
β at 3W1/m	6.83/3.49	10.4/ 3.51

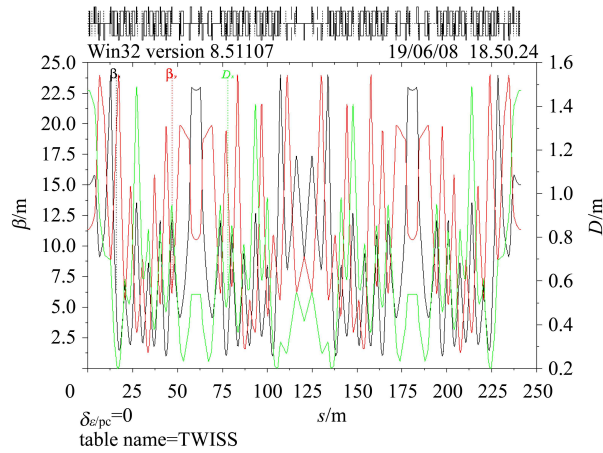


Fig. 3. The twiss parameters in the new mode.

3 Chromaticity correction and dynamic aperture optimization

3.1 Chromaticity correction

In order to have a large enough dynamic aperture, the sextupole strengths required by chromaticity correction should be optimized. For the dedicated SR mode, there is no mini- β insertion, compared with the collision mode. So we do not need to worry about the chromaticity above the 3rd order. Here, we use four families of sextupole to correct the chromaticity to the second order based on the interleaved method [1].

Like the BEPC II collision mode, nine sextupoles, labeled S1, S2, ..., S8 and S9 from the IP or the north crossing point (NCP) to the injection point in each arc, are used to correct the natural and higher order chromaticities. All of the 36 sextupoles are interleaved powered as four families, say SD1, SF1, SD2 and SF2. Here, SD and SF stand for defocusing and focusing sextupoles, respectively. To optimize the sextupoles, first we check the beta function at each sextupole. Because β_x is smaller than β_y at the focusing sextupole R4OS2, we switch off this sextupole. Then we use two families of sextupole to correct the first order chromaticity to +1 with the strength of 6.7 m^{-3} for all of the focusing sextupoles and -6.6 m^{-3} for all the defocusing sextupoles, and further calculate the effect of momentum deviation on beta function at each sextupole. Finally, we sort all of the sextupoles in to four families according to the disturbed beta function. By doing this, we can realize the second order chromaticity correction with the smallest adjustment of sextupole strengths, while keeping the first order chromaticity fixed. Table 2 shows the beta function of the off-momentum particles (δ is the energy deviation)

at each sextupole and how the sextupoles are sorted. The final sequence of the sextupole families is SD1, 0, SD1, SF1, SD2, SF2, SD1, SF1 and SD2 (corresponding to S1 to S9 in one arc). The strengths of the sextupoles, represented with the family names, are SD1 = -5.886399 m^{-3} , SF1 = 6.468807 m^{-3} , SD2 = -7.538448 m^{-3} and SF2 = 7.682361 m^{-3} , and the second and third chromaticities are $28.5/-7.8$ and $-489/324$, respectively, in the horizontal and vertical directions.

Table 2. The beta function perturbation.

SF family		$\beta_x(\delta=0.008)/\text{m}$	$\beta_y(\delta=0.008)/\text{m}$
SF1	S4	12.9	11.8
SF2	S6	7.5	8.3
SF1	S8	11.1	10.7
SD family		$\beta_x(\delta=0.008)/\text{m}$	$\beta_y(\delta=0.008)/\text{m}$
SD1	S1	22.4	24.0
SD1	S3	13.0	15.2
SD2	S5	8.9	7.6
SD1	S7	12.8	14.9
SD2	S9	18.8	18

3.2 Dynamic aperture optimization

After the linear lattice design and the chromaticity correction, we use the method of frequency map analysis (FMA) to analyze the dynamic aperture. Then we repeat the process of adjusting tunes, linear lattice matching, chromaticity correction and FMA several times to optimize the dynamic aperture. After the optimization, the working points are moved to $7.72/4.74$. The FMA results at the IP for the on-momentum particle before and after optimization are presented in Fig. 4. Fig. 5 is the dynamic aperture of on-momentum and off-momentum particles before and after the optimization.

We can see from the above two figures that the dynamic aperture is enlarged a little and the particles' transverse motion inside the dynamic aperture is more stable after optimization.

4 Compensation of the wigglers' linear effect

Because of the edge focusing of the wigglers, the beta function and the working point of the linear optics will be changed when the wigglers are inserted. We need to compensate this effect in order to avoid correcting the chromaticity again. In this paper, we use a hard-edge dipole model [2] based on the magnetic field measurement [2, 3] for wigglers and local matching method [4] to compensate the effects of wig-

glers. After compensation, the natural emittance increases to 91nm. Figs. 6 to 8 show the twiss parameters of the new lower emittance mode before and after the wiggler compensation.

ters of the new lower emittance mode before and after the wiggler compensation.

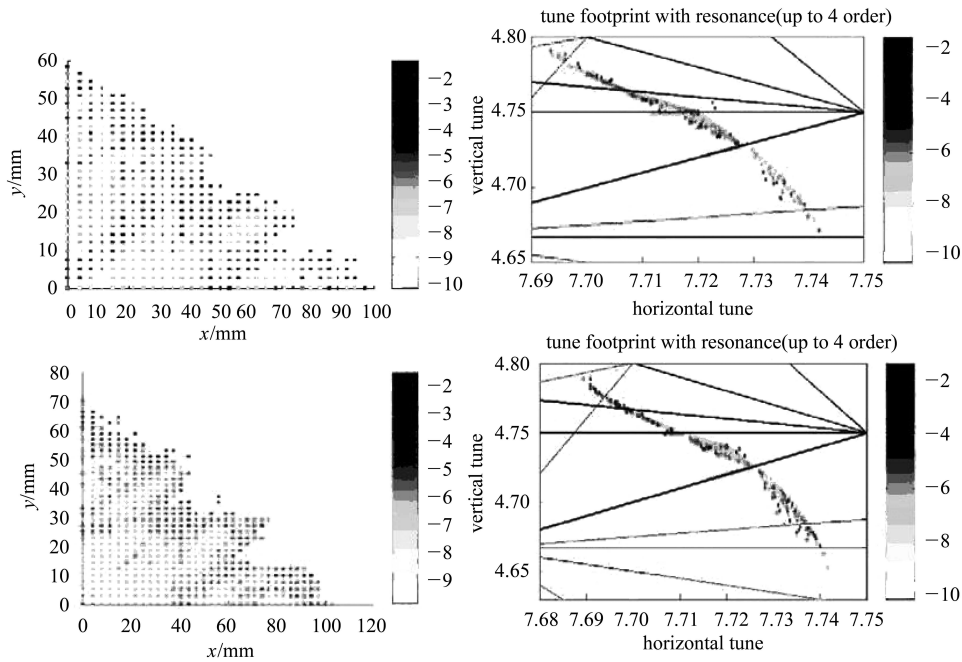


Fig. 4. FMA results at the IP for the on-momentum particle before and after optimization. (up: before, down: after).

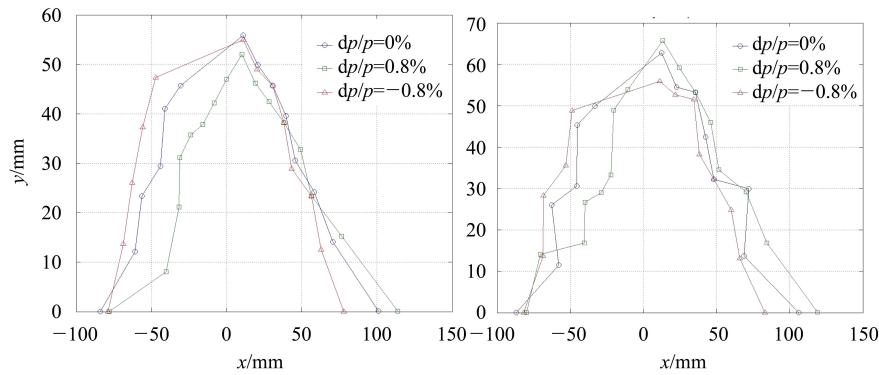


Fig. 5. Dynamic aperture at the IP for the on-momentum and off-momentum particles before and after optimization. (left: before, right: after).

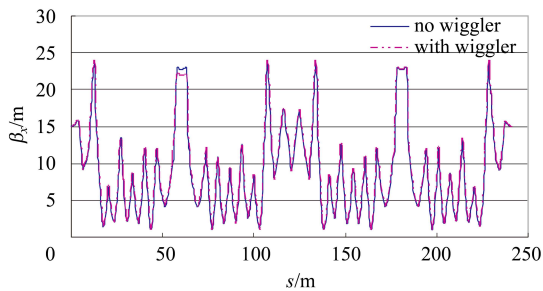


Fig. 6. Horizontal beta function of the new mode before and after the wiggler compensation.

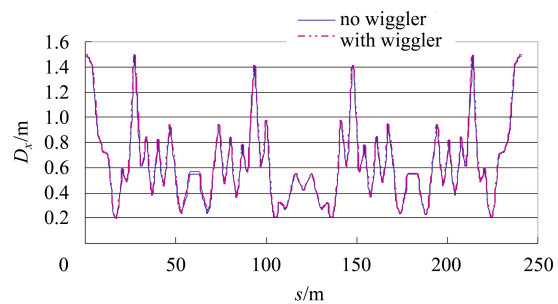


Fig. 7. Horizontal dispersion of the new mode before and after the wiggler compensation.

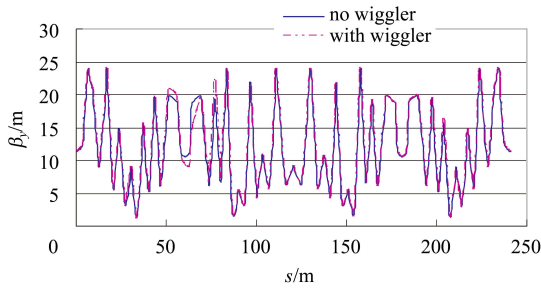


Fig. 8. Vertical beta function of the new mode before and after the wiggler compensation.

We can see that the twiss parameters of the new mode after the wiggler correction recover the original mode well, except for the injection region. The differences before and after the wiggler compensation are concentrated in the injection region because wigglers in this region are so close that there are not enough quadrupoles to correct their effects. Also, we can see that the wigglers' influences are mainly in the vertical direction rather than in the horizontal one.

5 Estimation of the wigglers' nonlinear influence on the dynamic aperture

As a main kind of nonlinear element, wigglers can degrade the dynamic aperture. We hope to estimate how much the dynamic aperture will be reduced because of the wigglers' nonlinear effect. We use an analytical method [5, 6] to calculate the dynamic aperture of the BEPC II with ideal non-linear wigglers. One has the dynamic aperture limited by a single wiggler as follows,

$$A_{N_w,y}(s) = \sqrt{\frac{3\beta_y(s)}{\beta_{y,m}^2} \frac{\rho_w}{k_y \sqrt{L_w}}}, \quad (2)$$

$$A_{N_w,x}(s) = \sqrt{\frac{\beta_y(s)}{\beta_x(s)} (A_{N_w,y}^2(s) - y^2)}, \quad (3)$$

where $\beta_x(s)$ and $\beta_y(s)$ are the unperturbed beta functions at a certain position, $\beta_{y,m}$ is the vertical beta function in the middle of the wiggler, $L_w = N_w \lambda_w$ is the total length of the wiggler, λ_w is the period length, and $k_y = k = 2\pi/\lambda_w$ where we have assumed plane poles. For the expression of the wiggler's magnetic field, $B_y = B_0 \cosh(k_y y) \cos(kz)$, the first nonlinear item about y in its expansion is an octupole component. So k_y can be looked as a nonlinear symbol in (2). Also, we can see that a shorter wiggler period λ_w will give a stronger nonlinear effect. In Formulae (2) and (3), the wiggler is an ideal model where the poles are plane and each of them is considered as a delta

function octupole. Then the total dynamic aperture of the whole wiggler is the collective contributions by an integration of all octupole components.

Assuming that the dynamic aperture of the ring without the wigglers' effects is A_y and that there are M wigglers to be inserted in the ring at different places, one has the total dynamic aperture by a special summary of the wigglers' effect and the sextupoles' effects,

$$A_{\text{total},y}(s) = \frac{1}{\sqrt{\frac{1}{A_y^2(s)} + \sum_{j=1}^M \frac{1}{A_{j,w,y}^2(s)}}}. \quad (4)$$

Using the above formula, the dynamic aperture at the IP including nonlinear wiggler effects for on-momentum particles is shown in Table 3.

Table 3. Dynamic aperture at the IP with the wigglers' non-linear effects.

	A_x/mm	A_y/mm
without wiggler	100	60
1W1 ($g=41$ mm)	66	77
1W2 ($g=41$ mm)	270	316
3W1 ($g=44$ mm)	216	252
4W1	229	267
4W2 ($g=18$ mm)	99	115
all wigglers	45	42

The first line in this table gives the dynamic aperture for the lattice without wigglers and the results from the second line to the sixth line are only for the individual wiggler. Then the last line gives the collective contribution from all of the magnets.

It can be seen that the dynamic aperture at the IP including the wigglers' effect is larger than the physical aperture. (The radius of the vacuum chamber at the IP is 31.5 mm [7], which is the smallest physical aperture in the SR ring.) So the dynamic aperture may not present a problem.

6 Routine operation with the new lattice

This low emittance SR mode ($\nu_x/\nu_y=7.72/4.74$) was tested primarily in December, 2008 and was used formally from October, 2009. The electron beam can be injected successfully with this mode, and it worked well in the last SR operation. However, the brightness of a few beam lines, such as 3W1 and 4B9, was decreased, even with this smaller emittance mode. The reason may come from the larger β function or larger dispersion at the synchrotron light extraction points.

So there are still some requirements for further optics optimization.

It needs to be pointed out that some quadrupoles' strengths have reached the limit so that we cannot increase their current further. This will present some operational difficulties for optics correction, which should be solved carefully.

7 Conclusion

In order to improve the brightness of the BEPC II as a light source, we study the lower emittance synchrotron radiation mode. The smallest emittance we get in this paper is 85 nm without wigglers and will be

91 nm while including wigglers. After the chromaticity correction and sextupole optimization, we can get a feasible dynamic aperture. Even with the wigglers' nonlinear effect, the dynamic aperture is still enough according to our analytical estimation and the real operation. This new mode has worked well in the last SR operation but further improvement based on this new mode is still needed to increase the brightness in some beam lines.

The authors would like to thank all of the colleagues of the BEPC II commissioning group for their helpful discussions and long-term support.

References

- 1 Verdier A. Chromaticity. CERN 95-06, 1995
- 2 Wiedemann H. Particle Accelerator Physics. Springer, 2007. 314
- 3 ZHOU D M. BEPC II Hard-edge Wiggler Modal Based on Magnetic Measurement. IHEP-AC-BEPCII-MD/2007-34 (in Chinese)
- 4 WANG D, QIN Q. BEPC II SR Mode Study with Wigglers. IHEP-AC-BEPC II-MD/2008-06 (in Chinese)
- 5 GAO J. Nucl. Instrum. Methods A, 2000, **451**: 545-557
- 6 GAO J. Nucl. Instrum. Methods A, 2004, **516**: 243-248
- 7 Chinese Academy of Sciences. Design Report for the Upgrade of BEPC. IHEP-BEPC II-SB-03-3, 2003.11 (in Chinese)